Applied Microbiology and Biotechnology (2018) 102:2051–2062
https://doi.org/10.1007/s00253-018-8746-6

MINI-REVIEW

D-lyxose isomerase and its application for functional sugar production

Jiawei Huang[1] · Ziwei Chen[1] · Wenli Zhang[1] · Tao Zhang[1,2] · Wanmeng Mu[1,2]

Received: 9 November 2017 / Revised: 26 December 2017 / Accepted: 27 December 2017 / Published online: 1 February 2018

Abstract

Functional sugars have attracted attention because of their wide application prospects in the food, cosmetics, and pharmaceutical industries in recent decades. Compared with complex chemical synthesis, enzymatic methods of creating functional sugars, characterized by high specificity, moderate reaction conditions, and sustainability, are favored. D-lyxose isomerase (D-LI, EC 5.3.1.15), an important aldose-ketose isomerase, catalyzes the reverse isomerization reaction between D-xylulose and D-lyxose, as well as D-fructose and D-mannose. D-LI has drawn researchers' attention due to its broad substrate specificity and high potential for enzymatic production of some functional sugars such as D-xylulose, D-mannose, and D-ribose. In this article, an overview of recent advances in the biochemical properties of various D-LIs is explored in detail. Structural analysis, active site identification, and catalytic mechanisms are also provided. Additionally, the applications of D-LIs for functional sugar production, including D-lyxose, D-mannose, and L-ribose, are reviewed in detail in this paper.

Keywords D-lyxose isomerase · D-lyxose · Substrate specificity · Functional sugar

Introduction

Currently, the incidence of chronic diseases such as diabetes, obesity, hyperlipidemia, and hypertension has increased rapidly throughout the world. These diseases are generally caused by the over intake of high sugar and high-fat foods. As a result, functional sugars with unique physiological benefits have attracted more public attention (Zhang et al. 2017b). These functional sugars can be chemically synthesized, but chemical synthesis methods usually have some drawbacks, including strict reaction conditions, complicated purification steps, chemical waste, and application safety issues (Bicas et al. 2010). Hence, the enzymatic conversion of functional sugars is preferred, because these methods can be more moderate, efficient, and sustainable. Prof. Izumori established a novel and complete strategy to synthesize rare sugars. Based on the Izumoring strategy, all the monosaccharides can be linked by enzymatic epimerization, isomerization, and oxidization-reduction, using ketose 3-epimerases, aldose isomerases, polyol dehydrogenases, and aldose reductase. In the past two decades, most studies on the production of rare sugars were based on this classical strategy (Izumori 2006).

D-lyxose isomerase (D-LI, EC 5.3.1.15) is an important aldose-ketose isomerase which can catalyze the reverse isomerization reaction between D-xylulose and D-lyxose, as well as D-fructose and D-mannose. Similar to L-rhamnose isomerase (EC 5.3.1.14) and L-ribose isomerase (EC 5.3.1.B3), D-LIs display broad substrate specificity for many functional aldoses and ketoses (Fig. 1) and have attracted much attention from researchers. As reported previously, D-LI plays an important role in the microbial catabolism of D-lyxose and L-ribose. First, D-lyxose and L-ribose are converted to D-xylulose and L-ribulose, respectively. After that, through catalysis of D-xylulokinase (EC 2.7.1.17) and L-ribulokinase (EC 2.7.1.16), D-xylulose and L-ribulose are transformed to D-xylulose 5-phosphate and L-ribulose 5-phosphate, which are common intermediates of the pentose phosphate pathway (Cho et al. 2007).

Because of their wide substrate specificity, D-LIs have been utilized for the production of functional sugars, such

Electronic supplementary material The online version of this article (https://doi.org/10.1007/s00253-018-8746-6) contains supplementary material, which is available to authorized users.

✉ Wanmeng Mu
wmmu@jiangnan.edu.cn

[1] State Key Laboratory of Food Science and Technology, Jiangnan University, Wuxi, Jiangsu 214122, China

[2] Synergetic Innovation Center of Food Safety and Nutrition, Jiangnan University, Wuxi 214122, China

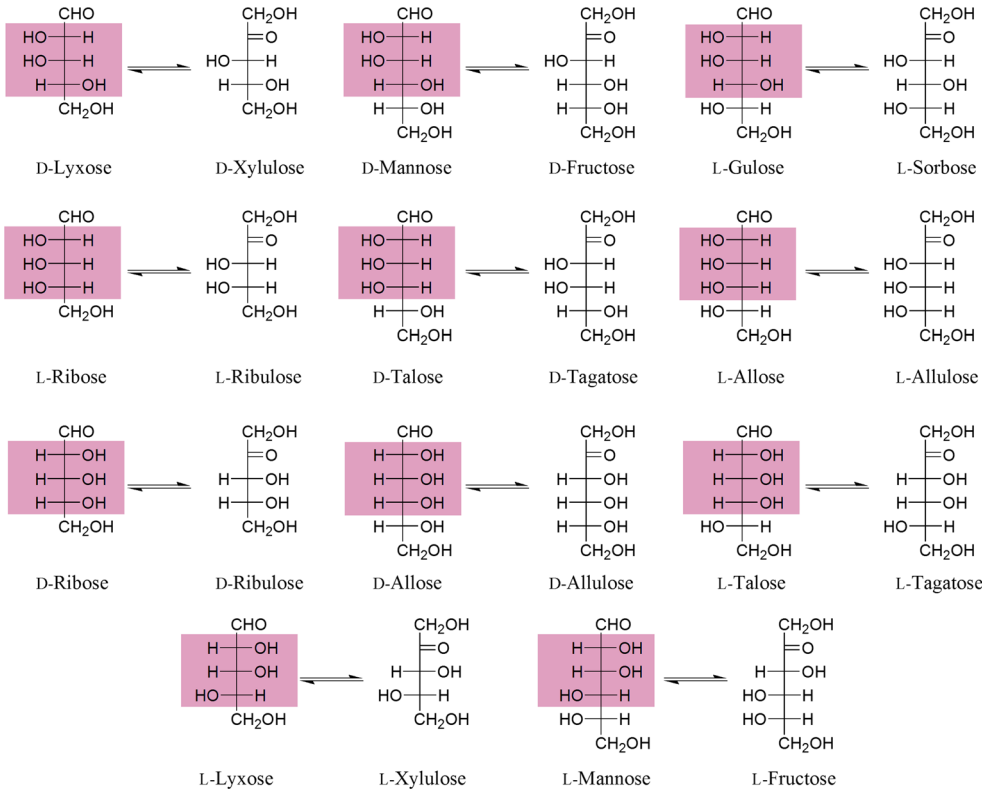

Fig. 1 A schematic diagram of aldose-ketose isomerization catalyzed by D-LIs. The pink boxed structures indicate the preferred hydroxyl configurations of C-2, C-3, and C-4. The activity orders are exhibited from the top to bottom in the figure

as D-lyxose, D-mannose, and some other L-form rare sugars like L-ribose and L-gulose. All these sugars have physiological functions. D-lyxose is a rare pentose, which is found in bacterial glycolipids, and is not usually utilized by microorganisms. It is often used as a precursor for immunostimulatory α-galactosylceramide and anti-tumor agents, a treatment for some murine cancers (Morita et al. 1996). D-Mannose is a natural hexose and the aldose isomer of D-fructose. It shows many health benefits, such as anti-diabetic function (Vuksan et al. 1999), prebiotic, and anti-inflammatory effects (Korneeva et al. 2012), and it is a treatment for phosphomannose isomerase deficiency (De and Seta 2009). In addition, D-mannose is an important precursor for the synthesis of D-mannitol (Mishra and Hwang 2013), vitamins (Chen et al. 2007), and anti-tumor and immunostimulatory agents (Zhang et al. 2017a). Because of the wide potential applications in pharmaceutical industry, L-sugars have also attracted much attention. L-ribose, the enantiomer of D-ribose, is commonly known as an intermediate of many L-nucleoside-based pharmaceutical compounds (Okano 2009).

Although D-LIs exhibit potential for functional sugar production, until now, there have been few reviews about D-LIs available. In this review, we focus on the recent advances in the biochemical properties and structural studies of D-LIs. In addition, the production of some functional sugars by D-LIs is also described in this review article.

Properties of various D-LIs

Novel enzyme sources

Several D-LIs have been isolated and characterized from different microorganisms. In 1965, the first characterized D-LI from *Aerobacter aerogenes* PRL-R3 was reported, which catalyzed the isomerization of D-lyxose and D-mannose and showed the best substrate specificity for D-lyxose (Anderson and Allison 1965). Thirty years later, the second D-LI was determined, which was isolated from *Cohnella laevoribosii* RI-39 (Cho et al. 2007). Recently, research on D-LI has been accelerated, and D-LIs have been identified and characterized from *Providencia stuartii* KCTC 2568 (Kwon et al. 2010), *Serratia proteamaculans* KCTC 2936 (Park et al. 2010b), *Escherichia coli* O157:H7 (Van et al. 2010), *Bacillus subtilis* strain 168 (Marles-Wright and Lewis 2011), *Bacillus licheniformis* DSM13 (Patel et al. 2011), *Dictyoglomus turgidum* DSM 6724 (Choi et al. 2012), and *Thermosediminibacter oceani* DSM 16646 (Yu et al. 2016). The isomerization capacities of different D-LIs are influenced by the microbial source and reaction conditions, such as pH, operation temperature, and metal ion cofactors. A summary of the enzymatic properties of the aforementioned D-LIs is shown in Table 1.

Table 1 Comparison of biochemical properties of various D-LIs

Microorganism	Optimum pH	Optimum temperature (°C)	Optimum metal, concentration	GenBank accession	Length (Aa)	Polymer	Subunit molecular mass (kDa)	Total molecular mass (kDa)	Half-life (h)	Highest production of D-lyxose (g L^{-1}) (temperature, pH, substrate)	Reference
C. laevoribosii	6.5	70	Mn^{2+}, 1 mM	ABI93960.1	182	dimer	21	42	NR[b]	NR	(Cho et al. 2007)
P. stuartii	7.5	45	Mn^{2+}, 1 mM	EDU58657	183	dimer	22	44	36 (30 °C) 14 (35 °C) 8.9 (40 °C) 3.4 (45 °C)1.4 (50 °C)	288 (45 °C, 7.5, 500 g L^{-1} D-xylulose)	(Kwon et al. 2010)
S. proteamaculans	7.5	40	Mn^{2+}, 1 mM	BAJ07463.1	228	dimer	27	54	84 (30 °C) 17 (35 °C) 2.6 (40 °C) 0.3 (45 °C) 0.09 (50 °C)	350 (40 °C, 7.0, 500 g L^{-1} D-xylulose)	(Park et al. 2010b)
E. coli	7.5	50	Mn^{2+}, 1 mM	Q8X5Q7	227	dimer	19.3	39	NR	NR	(Van et al. 2010)
B. licheniformis	7.5–8.0	40–45	Mn^{2+}, 1 mM	AAU22106.1	167	NR	19.5	NR	140 (30 °C) 62 (35 °C) 30 (40 °C) 18 (45 °C) 7 (50 °C)	NR	(Patel et al. 2011)
D. turgidum[a]	7.5	75	Co^{2+}, 1 mM	YP_002352606.1	181	dimer	22	44	9.1 (60 °C) 4.1 (65 °C) 2.8 (70 °C) 1.8 (75 °C) 0.8 (80 °C) 0.3 (85 °C)	380 (70 °C, 7.5, 500 g L^{-1} D-xylulose)	(Choi et al. 2012)
T. oceani	6.5	65	Mn^{2+}, 1 mM	ADL08607.1	181	dimer	22	44	12.7 (70 °C) 6.8 (75 °C) 1.7 (80 °C) 0.5 (85 °C)	NR	(Yu et al. 2016)

[a] The values were recalculated based on the original references after unit conversion

[b] *NR* not reported

Amino acid sequence comparison

Based on the identity comparison (Table S1), the D-LIs can be divided into two groups, namely group 1 and group 2. Group 1 contains *C. laevoribosii* D-LI (GenBank accession no. ABI93960.1, 182 aa), *P. stuartii* D-LI (EDU58657, 183 aa), *B. licheniformis* D-LI (AAU22106.1, 167 aa), *B. subtilis* D-LI (AIY91703, 167 aa), *D. turgidum* D-LI (YP_002352606.1, 181 aa), and *T. oceani* D-LI (ADL08607.1, 181 aa); their molecular weights are very similar, and they share 51.8 to 76.7% amino acid identity with each other. Group 2 contains *S. proteamaculans* D-LI (BAJ07463.1, 228 aa) and *E. coli* D-LI (Q8X5Q7, 227 aa); their molecular weights are much higher than all the D-LIs in group 1, and their amino acid identity is 71.4%. Despite the D-LIs share relatively high amino acid identity within each group, group 1 and group 2 exhibited very low amino acid identity with each other (20.6 to 29.1%). The phylogenetic tree of D-LIs confirmed these differences by species relationships as well (Fig. S1). Multiple amino acid sequences from various D-LIs were also aligned (Fig. 2) based on the structure of *E. coli* D-LI bounding with D-fructose; the active sites were identified (Van et al. 2010). Although the two groups share relatively low identity, the active site residues are strictly conserved among all these D-LIs, especially the residues related to metal coordination and substrate binding.

Effect of pH

Most of the reported D-LIs show optimal activity under weakly alkaline conditions of pH 7.5–8.0, including *P. stuartii* D-LI (Kwon et al. 2010), *S. proteamaculans* D-LI (Park et al. 2010b), *E. coli* D-LI (Van et al. 2010), *B. licheniformis* D-LI (Patel et al. 2011), and *D. turgidum* D-LI (Choi et al. 2012). Only *C. laevoribosii* D-LI and *T. oceani* D-LI had maximum activity levels at the slightly acidic conditions of pH 6.5 (Cho et al. 2007; Yu et al. 2016). Generally, acidic pH conditions are preferred in the industrial production of functional sugars (Bhosale et al. 1996; Lee et al. 2012) because non-enzymatic reactions of carbohydrates are inhibited in acidic conditions. Alkaline pH can accelerate non-enzymatic browning reactions, whereas the browning effect and unwanted by-products are reduced and suppressed in weakly acidic

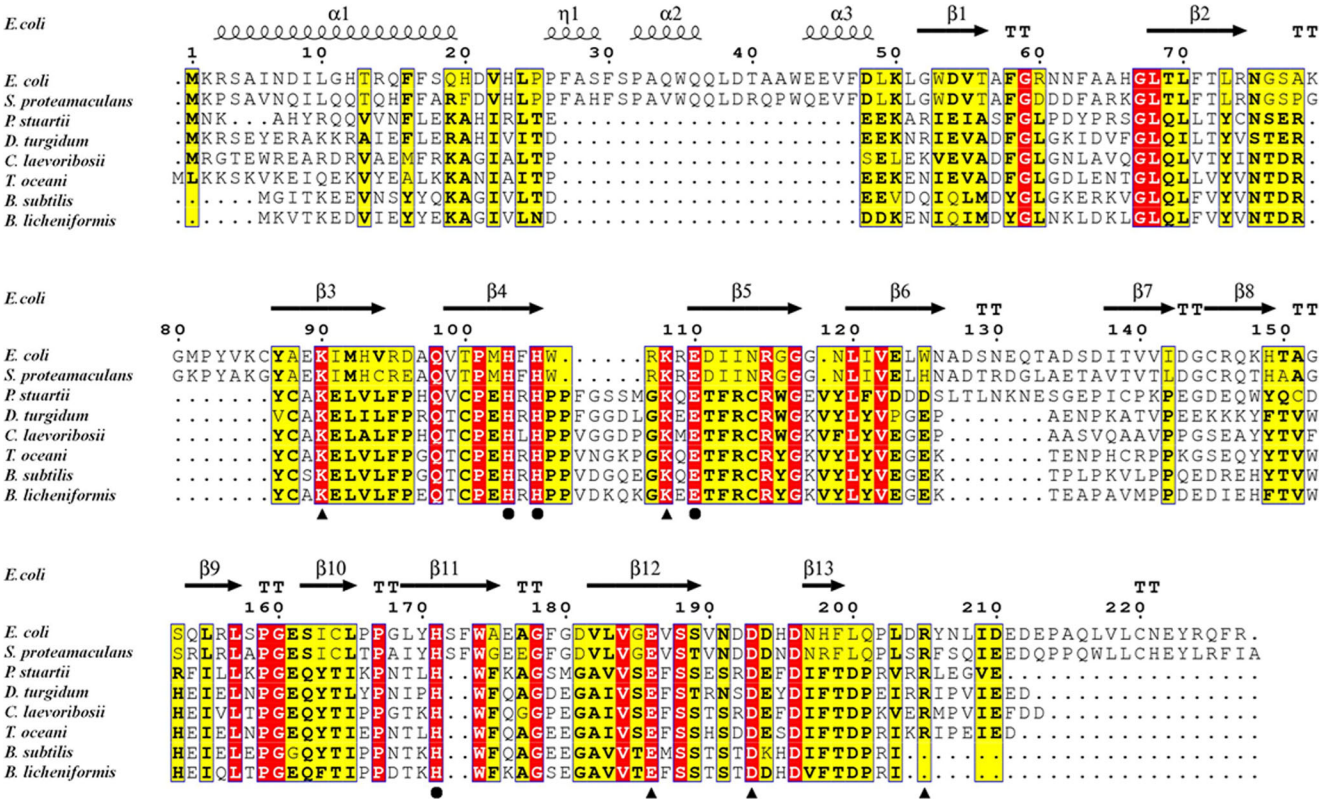

Fig. 2 Alignment of the amino acid sequences of various D-LIs. Residues related to substrate binding sites (black circle), and those involved in both the metal coordination and substrate binding sites (black triangle), according to the complex structure of *E. coli* D-LI bound to D-fructose (PDB no. 3MPB). The GenBank accession no. of D-LIs are as follows: *C. laevoribosii* D-LI (ABI93960.1), *P. stuartii* D-LI (EDU58657), *S. proteamaculans* D-LI (BAJ07463.1), *E. coli* D-LI (Q8X5Q7), *B. licheniformis* D-LI (AAU22106.1), *B. subtilis* D-LI (AIY91703), *D. turgidum* D-LI (YP_002352606.1), and *T. oceani* D-LI (ADL08607.1). The amino acid sequence of the *A. aerogenes* D-LI was not available from the NCBI GenBank. The alignment was carried out using the ESPript 3.0 service (http://espript.ibcp.fr/ESPript/ESPript/)

conditions (Friedman 1996; Shen and Wu 2010). Currently, many researchers are focusing on the screening, identification, and molecular modification of sugar isomerases with slightly acidic optimum pH, such as L-arabinose isomerases (EC 5.3.1.4) (Chen et al. 2015), D-glucose isomerases ((EC 5.3.1.5) (Bhosale et al. 1996), and D-psicose 3-epimerase (EC 5.3.1.15) (Zhang et al. 2015).

Effect of temperature

High operating temperatures are often needed for the industrial production of rare sugars because they can offer several advantages for the conversion of monosaccharides, such as fast reaction velocities, high substrate and product solubility, low viscosity, small risk of contamination, resistance to chemical denaturation, and shifting the equilibrium ratio towards endothermic reactions. When reaction temperature is high, the Maillard reaction occurred, which has merits such as excellent gel strength, emulsifying stability, foaming properties, and antioxidant activities. However, when temperature is too high, the Maillard reactions will be accelerated and may bring browning effects and other unwanted compounds. So, the proper temperature for industrial sugar production is 60–70 °C in order to control Maillard reaction (Mozhaev 1993; Xu et al. 2014). The optimal temperature for D-LI isomerization varies from 40 to 75 °C (Table 1). Among all the reported D-LIs, the thermostable *D. turgidum* D-LI showed the highest optimum temperature of 75 °C (Choi et al. 2012), whereas *S. proteamaculans* D-LI exhibited the lowest optimum temperature of 40 °C (Park et al. 2010b).

Thermostability is one crucial property related to the industrial application of D-LIs. Enzymes from *P. stuartii*, *S. proteamaculans*, and *B. licheniformis* exhibited relatively high thermostability at low temperatures, with half-lives ($t_{1/2}$) of 36, 84, and 140 h at 30 °C, respectively. However, at slightly higher temperatures, their thermostability drastically decreased, showing $t_{1/2}$ values of 1.4, 0.09, and 7 h at 50 °C, respectively (Kwon et al. 2010; Park et al. 2010b; Patel et al. 2011). *D. turgidum* D-LI showed relatively high thermostability, with $t_{1/2}$ values of 9.1, 4.1, 2.9, and 1.8 h at 60 to 75 °C (Choi et al. 2012). For *T. oceani* D-LI, the $t_{1/2}$ values were 12.7 and 7.8 h at 70 and 75 °C, respectively (Yu et al. 2016). It is interesting that the optimum temperature of *T. oceani* D-LI (65 °C) was lower than that of *D. turgidum* D-LI (75 °C), whereas its thermostability was much better at higher temperatures. The *T. oceani* D-LI displayed optimal activity and relatively high thermostability in acidic conditions (pH 6.5), suggesting that it has good potential in industrial applications. Patel et al. compared the amino acid content of different D-LIs and proposed that the higher stability of D-LI might be related to the high content of charged residues (Lys, Arg, Glu, and Asp) (Kumar et al. 2000) and low content of Asn and Gln residues (Patel et al. 2011).

Effect of metal ions

Based on the crystal structure, metal ions play a critical role in the catalytic mechanisms of D-LIs. Recent research characterizing various D-LIs has provided more evidence about the importance of metal ions. Different metal ions have various effects on the enzyme activity of D-LIs. In general, the presence of Mn^{2+} or Co^{2+} activates the D-LIs and enhances their catalytic efficiency several times to ten times. *A. aerogenes* D-LI and *C. laevoribosii* D-LI were identified as metal-dependent enzymes. For almost all the reported D-LIs, Mn^{2+} is considered to be the optimum metal ion for *A. aerogenes* D-LI (Anderson and Allison 1965), *C. laevoribosii* D-LI (Cho et al. 2007), *P. stuartii* D-LI (Kwon et al. 2010), *S. proteamaculans* D-LI (Park et al. 2010b), *E. coli* D-LI (Van et al. 2010), *B. licheniformis* D-LI (Patel et al. 2011), and *T. oceani* D-LI (Yu et al. 2016). Only for *D. turgidum* D-LI, the optimum metal ion is Co^{2+} (Choi et al. 2012). Interestingly, the presence of Co^{2+} can drastically inhibit the isomerization activity of *C. laevoribosii* D-LI and *P. stuartii* D-LI. The catalytic activities of many sugar enzymes, such as L-arabinose isomerase (Xu et al. 2014), ketose 3-epimerase (Zhang et al. 2016), L-rhamnose isomerase (Xu et al. 2016a), and D-glucose isomerase (Bock et al. 1983), are influenced by divalent cations, especially Mn^{2+} and Co^{2+}. In addition, metal ions are related to the stability of some other sugar enzymes. For example, the thermostability and structural stability of D-psicose 3-epimerase and L-rhamnose isomerase are improved by the addition of metal ions (Chen et al. 2017; Zhang et al. 2013).

Substrate specificity and kinetic parameters

The kinetic parameters of D-LIs are another important factor for industrial application. The kinetic parameters of the abovementioned D-LIs are compared in Table 2. With D-lyxose as the substrate, *A. aerogenes* D-LI exhibited the lowest K_m value (3.6 mmol L^{-1}), whereas *P. stuartii* D-LI exhibited the highest K_m value (47.0 mmol L^{-1}). With D-xylulose as the substrate, *S. proteamaculans* D-LI exhibited the lowest K_m value (3.8 mmol L^{-1}), whereas *P. stuartii* D-LI also exhibited the highest K_m value (38.0 mmol L^{-1}). In addition, *B. licheniformis* D-LI showed the highest specific activity for D-lyxose (54.0 U mg^{-1}), which was much higher than other reported D-LIs. *E. coli* D-LI showed the lowest specific activity for D-lyxose (5.8 U mg^{-1}). Additionally, the equilibrium ratio between D-xylulose and D-lyxose was compared. The equilibrium ratio for *A. aerogenes* D-LI and *D. turgidum* D-LI was nearly 20:80, whereas the highest equilibrium ratio for *C. laevoribosii* D-LI was nearly 65:35.

Similar to L-rhamnose isomerase and L-ribose isomerase (Xu et al. 2016a, b), D-LIs also displayed broad substrate specificity for many aldoses and ketoses. The substrate specificity of various D-LIs is compared in Table 3. Among the

Table 2 Comparison of kinetic parameters of various D-LIs

Microorganism	Equilibrium ratio between D-xylulose and D-lyxose	Specific activity (U mg^{-1})[c]	k_{cat} (s^{-1})		K_m (mmol L^{-1})		k_{cat}/K_m (s^{-1} mmol L^{-1})		Reference
			D-lyxose	D-xylulose	D-lyxose	D-xylulose	D-lyxose	D-xylulose	
A. aerogenes	19:81 (25 °C)	7.7	NR	NR	3.6	NR	NR	NR	(Anderson and Allison 1965)
C. laevoribosii	49:51 (60 °C)	13.4	1902	NR	22.4	NR	84.9	NR	(Cho et al. 2007)
P. stuartii	42:58 (45 °C)	22.3	31.340	34.960	47.0	38.0	669	920	(Kwon et al. 2010)
S. proteamaculans	30:70 (40 °C)	10.0	30.810	31.620	13.3	3.8	2333	9560	(Park et al. 2010b)
E. coli	NR[b]	5.8	13.7	NR	16.1	NR	850	NR	(Van et al. 2010)
B. licheniformis	65:35 (40 °C)	54.0	98	NR	30.4	NR	3.2	NR	(Patel et al. 2011)
D. turgidum [a]	15:85 (30 °C)	18.8	214.200	249.600	39.0	5.0	5460	55.200	(Choi et al. 2012)
	17:83 (40 °C)								
	18:82 (50 °C)								
	19:81 (60 °C)								
	20:80 (70 °C)								
	22:78 (80 °C)								
T. oceani[a]	NR	7.1	186.480	NR	15.5	NR	12.060	NR	(Yu et al. 2016)

[a] The values were recalculated based on the original references after unit conversion

[b] *NR* not reported

[c] One unit (U) is defined as the D-LI amount producing 1 μmol D-xylulose from D-lyxose per minute

aldose substrates, the optimum substrate for D-LIs was D-lyxose followed by D-mannose. For all characterized D-LIs, the substrate specificity for ketoses was higher than the corresponding aldoses. No activity was detected with aldose phosphates as the substrate (Choi et al. 2012). According to previous studies and summarized in Fig. 1, D-LIs displayed very high substrate specificity for aldoses with the C-2 and C-3 hydroxyl groups oriented in the left-hand configuration and the C-4 hydroxyl group oriented in the right-hand configuration (Fischer projections (D-lyxose, D-mannose and L-gulose)). When the hydroxyl groups of C-2, C-3, and C-4 were oriented in the left-hand configuration, D-LIs showed relatively high substrate specificity for the aldoses L-ribose, D-talose, and D-allose. If the C-2, C-3, and C-4 hydroxyl groups were oriented in the right-hand configuration, the substrate specificity for these aldoses (D-ribose, D-allose and L-talose) was low. Finally, D-LIs exhibited very little or nearly null activity for the aldoses L-mannose and L-lyxose, which have the C-2 and C-3 hydroxyl groups oriented in the right-hand configuration and the C-4 hydroxyl group oriented in the left-hand configuration (Kwon et al. 2010; Van et al. 2010). Among all the D-LIs, *B. licheniformis* D-LI displayed the highest specific activities for several substrates, such as D-lyxose (54.0 U mg^{-1}), D-mannose (41.0 U mg^{-1}), D-xylulose (78.0 U mg^{-1}), and L-ribulose (12.0 U mg^{-1}), indicating that *B. licheniformis* D-LI might be very suitable for the production of these functional sugars (Choi et al. 2012).

Crystal structure and catalytic mechanism

Overall structures

To date, only two crystal structures of D-lyxose isomerase have been solved and released, including D-LI from *E. coli* O157:H7 (Protein Data Bank, PDB no. 3KMH) and D-LI from *B. subtilis* strain 168 (PDB no. 2Y0O; Marles-Wright and Lewis 2011; Van et al. 2010). Both *E. coli* D-LI and *B. subtilis* D-LI assemble into a dimeric structure in the asymmetric unit. *E. coli* D-LI belongs to the cupin protein superfamily, and its overall structure is the typical cupin β-barrel fold, with a 20-residue α-helix and three shorter α-helices at the N-terminus. The helices are followed by the cupin domain, which consists of two anti-parallel β-sheets. Both the metal ion-binding site and substrate-binding site are located in a deep hydrophobic pocket formed by the β-barrels. The buried dimerization interface accounts for 14.3% of the total solvent-accessible area of *E. coli* D-LI. The two subunits are intimately connected by the disulfide bond formed by two Cys86, one from each peptide chain. In addition, the dimerization is further facilitated by the extensive hydrogen-bonding network, which includes 20 hydrogen bonds and 15 intermolecular salt bridges (Van et al. 2010). Although

Table 3 Specific activities (U mg^{-1}) of various D-LIs for different substrates[a]

Substrate	Product	*C. laevoribosii*	*P. stuartii*[b]	*S. proteamaculans*	*E. coli*	*B. licheniformis*	*D. turgidum*[b]	*T. oceani*
Aldose								
D-lyxose	D-xylulose	13.4	22.330	10.0	5.80	54	18.800	7.1
D-mannose	D-fructose	0.8	0.523	5.42	4.73	41	1.668	5.3
L-gulose	L-sorbose	NR [c]	NR	1.05	1.55	NR	NR	NR
L-ribose	L-ribulose	0.1	0.219	0.14	0.095	NR	0.119	NR
D-talose	D-tagatose	NR	0.045	0.19	0.20	NR	0.106	NR
L-allose	L-allulose	NR	0.022	NR	0.01	NR	0.008	NR
D-ribose	D-ribulose	ND[d]	0.014	NR	NR	NR	NR	NR
D-allose	D-allulose	NR	0.013	NR	NR	NR	NR	NR
L-talose	L-tagatose	NR	0.011	NR	NR	NR	NR	NR
L-lyxose	L-xylulose	ND	0.007	NR	NR	NR	NR	NR
L-mannose	L-fructose	NR	0.003	NR	NR	NR	NR	NR
Ketose								
D-xylulose	D-lyxose	NR	24.040	26.2	35.2	78	33.100	NR
L-ribulose	L-ribose	NR	0.872	0.40	0.18	NR	0.292	NR
D-fructose	D-mannose	NR	0.403	1.41	1.19	12	0.094	1.2
L-xylulose	L-lyxose	NR	0.180	NR	NR	NR	NR	NR
D-ribulose	D-ribose	NR	0.096	NR	NR	NR	0.077	NR
L-fructose	L-mannose	ND	0.017	NR	NR	NR	NR	NR
L-sorbose	L-gulose	NR	NR	NR	0.024	NR	NR	NR
D-tagatose	D-talose	NR	0.015	0.28	0.006	NR	0.022	NR
L-allulose	L-allose	NR	0.010	NR	0.0004	NR	NR	NR
D-allulose	D-allose	NR	0.005	NR	NR	NR	NR	NR
L-tagatose	L-talose	NR	0.002	0.02	NR	NR	NR	NR
Reference		(Cho et al. 2007)	(Kwon et al. 2010)	(Park et al. 2010b)	(Van et al. 2010)	(Patel et al. 2011)	(Choi et al. 2012)	(Yu et al. 2016)

[a] One unit (U) is defined as the enzyme amount producing 1 μmol product from substrate per minute

[b] The values were recalculated based on the original references after unit conversion

[c] *NR* not reported

[d] *ND* not determined

the amino acid identity between *B. subtilis* D-LI and *E. coli* D-LI is low (24%), their structures are very similar. Their monomer structures are shown superimposed in Fig. 3. *B. subtilis* D-LI also forms a cupin β-barrel structure. Two α-helices are located at the N-terminus, and two anti-parallel β-sheets follow the α-helices to form the cupin domain. The active pocket is also located in a domain between these β-sheets. *B. subtilis* D-LI forms a dimeric structure, and the interface is composed of the first β-sheet and a loop region between the α-helices at the N-terminus. The interface is stabilized by 8 salt bridges and 16 hydrogen bonds between subunits, which accounts for 13% of the overall accessible surface (Marles-Wright and Lewis 2011).

Metal coordination sites

In the crystal structure of *E. coli* D-LI, the metal coordination sites are located in the deep hydrophobic pocket formed by the β-barrel. The manganese ions (Mn^{2+}) are being coordinated by two water molecules and four residues (H103, H105, H171, and E110), which are completely conserved across all D-LIs. Interestingly, because the pocket in the cupin domain is too deep, the metal binding affinity of the protein is tight, and EDTA treatment fails to chelate the metal ions (Van et al. 2010). For *B. subtilis* D-LI, there are two metal ions in the active sites, including zinc (Zn^{2+}) and arsenic (As^{3+}) ions. Similar to *E. coli* D-LI, the primary binding ion (Zn^{2+}) of *B. subtilis* D-LI is also coordinated by two water molecules and four strictly conserved residues (H69, H71, H137, and E82). However, the coordination for this metal site appears to be suboptimal for zinc (Van et al. 2010), and the metal binding site might be configured optimally for manganese (Harding 2006). From the amino acid sequence alignment (Fig. 2), these three histidines and one glutamic acid residue, which are related to metal binding sites, are strictly conserved among all the reported D-LIs.

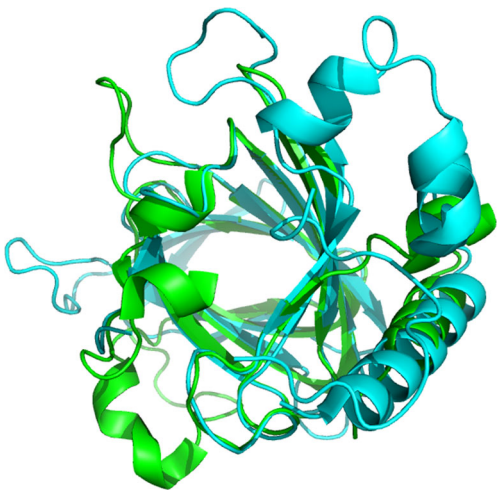

Fig. 3 Superimposition of the monomer of *E. coli* D-LI (cyan) and *B. subtilis* D-LI (green). The PDB structures of *E. coli* D-LI and *B. subtilis* D-LI are no. 3MPB and no. 2Y0O, respectively. The subunit superimposition was performed in PyMol

Substrate binding sites

Only the structure of the *E. coli* D-LI complex with D-fructose bound has been solved (PDB no. 3MPB). The complex structure of *E. coli* D-LI is quite similar to the apo structure overall. From the structure complexed with D-fructose, the substrate D-fructose is bound by K90, K108, E110, E186, D193, and N197 by hydrogen bond interactions, as well as by the Mn^{2+} ion. In the well-ordered molecule B, R205, located in the loop between residues L203 and L208, was also found to interact with the O-4 positions of D-fructose by hydrogen bonding (Van et al. 2010).

Van et al. also performed alanine-scanning mutagenesis around potential key residues in the active site, including K90, K108, E110, E186, D193, N197, and R205. The mutation E110A, which is involved in both metal coordination and substrate binding, results in a sharp decrease in enzyme activity. Additionally, the mutations of K108A, E186A, and D193A led to a complete loss of catalytic activity. Residue K108 is related with O-2 of D-fructose, whereas residue E186 might improve the chemical characteristics of the active pocket and enhance the stabilization with K108. Although residues D193 and K90 form interactions with hydroxyl groups not involved in isomerization, they play a key role in the optimal orientation of the substrate. Based on the structures, residue R205 was related to substrate specificity. Interestingly, the R205A mutation only shows catalytic activity towards D-lyxose (Van et al. 2010). As displayed in Fig. 2, all these residues involved in D-fructose binding were strictly conserved among all the reported D-LIs. Only residue N917, which forms interactions with the O-2 of D-fructose by hydrogen bonding, was not conserved. The mutation analysis corresponds with the sequence alignment results.

Catalytic mechanism

Based on the crystal structure and mutation results for the key residues in the active site of *E. coli* D-LI, Van et al. proposed a cis-enediolate-based mechanism. The natural form of monosaccharides in solution is the closed ring form (Swenson and Barker 1971). The histidine residue (H103), which might not only coordinate the metal ions but could also be positioned near the O-5 of the D-fructose and available for hydrogen bonding, is supposed to be used as an acid catalyst for ring opening. Once the ring is opened, another metal binding residue, E110, immediately abstracts the proton, and a cis-enediol intermediate is formed. The cis-enediol intermediate is not very stable, so isomerization occurs. The subsequent stabilization is facilitated by the positively charged residue

K108. During the isomerization process, R205 located in the loop region can form interactions with the hydroxyl group of C-4, which might block solvent entry and close the active pocket. After the isomerization process, the loop changes to the open conformation, allowing the product to be released and a new substrate molecule to bind (Van et al. 2010).

Recently, molecular modification technologies, including site-directed mutagenesis, random mutagenesis, high-throughput screening (HTS), and directed evolution, have developed quickly and have been extensively used to improve the catalytic activity, thermostability, substrate specificity, and pH optimum of enzymes. Some sugar enzyme variants with desirable properties have already been obtained, such as D-glucose isomerase (Hartley et al. 2000), L-arabinose isomerase (Lee et al. 2012), and D-psicose 3-epimerase (Bosshart et al. 2013, 2015). Although the crystal structures and catalytic mechanism of D-LI have been solved, there is still no similar application for D-LI. Performing the molecular modification on these enzymes in the future is urgently needed.

Bioproduction of functional sugars by D-LIs

Production of D-lyxose

D-lyxose is usually regarded as the precursor for immunostimulatory α-galactosylceramide and anti-tumor agents, which can be used for treating some murine cancers (Morita et al. 1996; Yasushi Takagi et al. 1996). Until now, several D-LIs have been used for large-scale D-lyxose production from D-xylulose. Using 500 g L^{-1} D-xylulose as the substrate, *P. stuartii* D-LI can produce 288 g L^{-1} D-lyxose in 2 h, at pH 7.5 and 45 °C, with a conversion yield of 58% and a volumetric productivity of 144 g L^{-1} h^{-1} (Kwon et al. 2010). For *S. proteamaculans* D-LI, 35% (*w*/*v*) D-lyxose can be obtained from 50% (*w*/*v*) D-xylulose in 3 h, at pH 7.5 and 35 °C, with a conversion yield of 70% and a productivity of 117 g L^{-1} h^{-1} (Park et al. 2010b). After reaction optimization, *D. turgidum* D-LI could yield 380 g L^{-1} D-lyxose from 500 g L^{-1} D-xylulose in 2 h, at pH 7.5 and 70 °C, with a conversion yield of 76% and the highest productivity of 190 g L^{-1} h^{-1}. The reaction temperature can influence the equilibrium ratio of *D. turgidum* D-LI, and the reaction shifted to the production of D-xylulose with an increase in temperature (Choi et al. 2012). Due to the broad substrate specificity of mannose-6-phosphate isomerase, this enzyme can also convert D-xylulose to D-lyxose (Yeom et al. 2009). Ahmed et al. also reported the production of D-lyxose from D-glucose by a three-step reaction combination. First, D-glucose is catalyzed to D-arabitol, and then D-arabitol is almost completely converted to D-xylulose by two different microorganisms. Finally, D-xylulose is isomerized to D-lyxose by L-ribose isomerase (Ahmed et al. 1999).

Production of D-mannose

D-mannose is not only the epimer of D-glucose at C-2 position but also the aldose isomer of D-fructose (Hu et al. 2016). It has great economic and application value in food, cosmetics, and pharmaceutical industries. D-mannose is most commonly produced from D-fructose by D-mannose isomerase, with an approximately conversion yield of 35%. Recently, due to the wide substrate specificity, some D-LIs have also been used for D-mannose production. By using purified *S. proteamaculans* D-LI, 10% (*w*/*v*) D-mannose was produced from 50% (*w*/*v*) D-fructose in 5 h, at pH 7.5 and 35 °C, with a conversion yield of 20% and a productivity of 20 g L^{-1} h^{-1} (Park et al. 2010b). Using 600 g/L D-fructose as the substrate, 150 g/L D-mannose was obtained by free *P. stuartii* D-LI in 2 h at pH 7.5 and 35 °C. After immobilization on Duolite A568 beads, the immobilized *P. stuartii* D-LI in 300 g/L D-fructose yielded 75 g L^{-1} h^{-1} D-mannose with a conversion yield of 25% after 23 cycles (Park et al. 2010a). From 400 g/L D-fructose, the thermostable *T. oceani* D-LI produced 101.6 g/L D-mannose at pH 6.5 and 60 °C with a conversion yield of 25.4% (Yu et al. 2016). Patel et al. proposed the two-step approach for D-mannose production from D-glucose by coupling D-glucose isomerase and D-LI (Patel et al. 2011). It has also been reported that the cellobiose 2-epimerase from *Caldicellulosiruptor saccharolyticus* catalyzed the epimerization of D-glucose to D-mannose directly. Using 500 g L^{-1} D-glucose as the substrate, it produced approximately 47.5 g L^{-1} D-fructose and 75 g L^{-1} D-mannose. The overall conversion yield of D-mannose from D-glucose reached 15%, and the equilibrium ratio of D-glucose, D-fructose, and D-mannose catalyzed by *C. saccharolyticus* 2-CE was approximately 75.5:9.5:15 (Park et al. 2011).

Production of L-ribose

L-ribose, a rare sugar, is the enantiomer of D-ribose. It is often used as a key intermediate for the synthesis of many L-nucleoside-based anti-viral drugs against human immunodeficiency virus, cytomegalovirus, and hepatitis virus (Okano 2009). As a result, enzymatic production for L-ribose is urgently needed. L-ribose can be synthesized from L-ribulose by L-ribose isomerase or mannose-6-phosphate isomerase, but L-ribulose is also very scarce and expensive (Xu et al. 2016b). Usually, L-ribose production is carried out in a two-step reaction from L-arabinose by L-arabinose isomerase and mannose-6-phosphate isomerase (Kim et al. 2014). Recently, Patel et al. reported the two-step isomerization process for L-ribose production using L-arabinose isomerase and D-lyxose isomerase. First, L-arabinose was transformed to L-ribulose as an intermediate by L-arabinose isomerase from *Shigella flexneri*. Then, L-ribulose was converted to L-ribose by *C. laevoribosii* D-LI. The overall conversion yield of L-ribose from L-

arabinose was 25%, and the equilibrium ratio of L-arabinose, L-ribulose and L-ribose reached 1.6:5.9:2.5 (Patel et al. 2017). M. Helanto et al. introduced an L-ribose isomerase into L-ribulokinase-deficient mutants of *E. coli* and *L. plantarum* and used these mutants for the production of L-ribose from L-arabinose. The initial L-ribose production rates at 39 °C and pH 8 were 0.46 g g^{-1} h^{-1} (1.84 g L^{-1} h^{-1}) and 0.27 g g^{-1} h^{-1} (1.91 g L^{-1} h^{-1}) for *E. coli* and for *L. plantarum*, respectively. Conversions of L-arabinose to L-ribose were 19.7 and 20% for *E. coli* and for *L. plantarum*, and their initial L-ribose production rates at 39 °C and pH 8 were 0.46 g g^{-1} h^{-1} (1.84 g L^{-1} h^{-1}) and 0.27 g g^{-1} h^{-1} (1.91 g L^{-1} h^{-1}), respectively (Helanto et al. 2009). The whole cell reaction has more advantages than the enzymatic production of sugars because it can simplify the purification process and improve assembly efficiency (Johnston et al. 2000), and it may also reduce the harm of external environmental factors and render the enzyme more stable (Ishige et al. 2005). It may also be possible to reach even higher yields using whole cells since the reaction takes place in the cytoplasm and the products can be transported into the medium (Helanto et al. 2009). Borate can form more stable complexes with ketoses than aldoses, so borate supplementation might shift the conversion rate towards production, a strategy that has already been used for the production of D-tagatose, D-allulose, and L-ribulose (Kim et al. 2008; Lim et al. 2007; Xu et al. 2016a). In addition, the development of simulated moving bed (SMB) chromatography improved the separation between different isomers, which might be applied to industrial production of rare sugars (Long et al. 2009; Wagner et al. 2015).

Funding information This study was funded by the NSFC Project (no. 21276001), the 863 Project (no. 2013AA102102), the Support Project of Jiangsu Province (no. BK20130001 and 2015-SWYY-009), and the project of Outstanding Scientific and Technological Innovation Group of Jiangsu Province (Jing Wu).

Compliance with ethical standards

Conflict of interest The authors declare that they have no conflict of interest.

Ethical approval This article does not contain any studies with human participants or animals performed by any of the authors.

References

Ahmed Z, Sasahara H, Bhuiyan SH, Saiki T, Shimonishi T, Takada G, Izumori K (1999) Production of D-lyxose from D-glucose by microbial and enzymatic reactions. J Biosci Bioeng 88(6):676–678. https://doi.org/10.1016/S1389-1723(00)87100-5

Anderson RL, Allison DP (1965) Purification and characterization of D-lyxose isomerase. J Biol Chem 240(8):2367–2372

Bhosale SH, Rao MB, Deshpande VV (1996) Molecular and industrial aspects of glucose isomerase. Microbiol Rev 60(2):280–300

Bicas JL, Silva JC, Pastore GM (2010) Biotechnological production of bioflavors and functional sugars. Cienc Tecnol Aliment 30(1):7–18

Bock K, Meldal M, Meyer B, Wiebe L (1983) Isomerization of D-glucose with glucose-isomerase. A mechanistic study. Acta Chem Scand 37(2):101–108

Bosshart A, Hee CS, Bechtold M, Schirmer T, Panke S (2015) Directed divergent evolution of a thermostable D-tagatose epimerase towards improved activity for two hexose substrates. Chembiochem 16(4): 592–601. https://doi.org/10.1002/cbic.201402620

Bosshart A, Panke S, Bechtold M (2013) Systematic optimization of interface interactions increases the thermostability of a multimeric enzyme. Angew Chem Int Edit 125(37):9855–9858

Chen F, Wei X, Tao Z, Zhou L, Bo J, Mu W (2015) Engineering of *Alicyclobacillus hesperidum* L-arabinose isomerase for improved catalytic activity and reduced pH optimum using random and site-directed mutagenesis. Appl Biochem Biotechnol 177(7):1480–1492

Chen F, Zhao J, Xiong F, Xie B, Zhang P (2007) An improved synthesis of a key intermediate for (+)-biotin from D-mannose. Carbohydr Res 342(16):2461–2464. https://doi.org/10.1016/j.carres.2007.06.029

Chen Z, Xu W, Zhang W, Zhang T, Jiang B, Mu W (2017) Characterization of a thermostable recombinant L-rhamnose isomerase from *Caldicellulosiruptor obsidiansis* OB47 and its application for the production of L-fructose and L-rhamnulose. J Sci Food Agric. https://doi.org/10.1002/jsfa.8703

Cho EA, Lee DW, Cha YH, Lee SJ, Jung HC, Pan JG, Pyun YR (2007) Characterization of a novel D-lyxose isomerase from *Cohnella laevoribosii* RI-39 sp. nov. J Bacteriol 189(5):1655–1663. https://doi.org/10.1128/JB.01568-06

Choi JG, Hong SH, Kim YS, Kim KR, Oh DK (2012) Characterization of a recombinant thermostable D-lyxose isomerase from *Dictyoglomus turgidum* that produces D-lyxose from D-xylulose. Biotechnol Lett 34(6):1079–1085. https://doi.org/10.1007/s10529-012-0874-y

De LP, Seta N (2009) The clinical spectrum of phosphomannose isomerase deficiency, with an evaluation of mannose treatment for CDG-Ib. BBA-M Basis Dis 1792(9):841–843

Friedman M (1996) Food browning and its prevention: an overview. J Agric Food Chem 44(3):631–653. https://doi.org/10.1021/jf950394r

Harding MM (2006) Small revisions to predicted distances around metal sites in proteins. Acta Crystallogr 62(6):678–682

Hartley BS, Hanlon N, Jackson RJ, Rangarajan M (2000) Glucose isomerase: insights into protein engineering for increased thermostability. BBA Protein Struct Mol Enzym 1543(2):294–335. https://doi.org/10.1016/S0167-4838(00)00246-6

Helanto M, Kiviharju K, Granström T, Leisola M, Nyyssölä A (2009) Biotechnological production of L-ribose from L-arabinose. Appl Microbiol Biotechnol 83(1):77–83. https://doi.org/10.1007/s00253-008-1855-x

Hu X, Shi Y, Zhang P, Miao M, Zhang T, Jiang B (2016) D-mannose: properties, production, and applications: an overview. Compr Rev Food Sci F 15(4):773–785. https://doi.org/10.1111/1541-4337.12211

Ishige T, Honda K, Shimizu S (2005) Whole organism biocatalysis. Curr Opin Chem Biol 9(2):174–180. https://doi.org/10.1016/j.cbpa.2005.02.001

Izumori K (2006) Izumoring: a strategy for bioproduction of all hexoses. J Biotechnol 124(4):717–722. https://doi.org/10.1016/j.jbiotec.2006.04.016

Johnston K, Clements A, Venkataramani RN, Trievel RC, Marmorstein R (2000) Coexpression of proteins in bacteria using T7-based expression plasmids: expression of heteromeric cell-cycle and transcriptional regulatory complexes. Protein Expr Purif 20(3):435–443. https://doi.org/10.1006/prep.2000.1313

Kim KR, Seo ES, Oh DK (2014) L-ribose production from L-arabinose by immobilized recombinant *Eescherichia coli* co-expressing the L-arabinose isomerase and mannose-6-phosphate isomerase genes from *Geobacillus thermodenitrificans*. Appl Biochem Biotechnol 172(1):275–288. https://doi.org/10.1007/s12010-013-0547-x

Kim NH, Kim HJ, Kang DI, Jeong KW, Lee JK, Kim Y, Oh DK (2008) Conversion shift of D-fructose to D-psicose for enzyme-catalyzed epimerization by addition of borate. Appl Environ Microbiol 74(10):3008–3013. https://doi.org/10.1128/AEM.00249-08

Korneeva OS, Cheremushkina IV, Glushchenko AS, Mikhaĭlova NA, Baturo AP, Romanenko ÉE, Zlygostev SA (2012) Prebiotic properties of mannose and its effect on specific resistance. Zhurnal Mikrobiol Epidemiol Immunobiol 5:67–70

Kumar S, Tsai CJ, Nussinov R (2000) Factors enhancing protein thermostability. Protein Eng 13(3):179–191. https://doi.org/10.1093/protein/13.3.179

Kwon HJ, Yeom SJ, Park CS, Oh DK (2010) Substrate specificity of a recombinant D-lyxose isomerase from *Providencia stuartii* for monosaccharides. J Biosci Bioeng 110(1):26–31. https://doi.org/10.1016/j.jbiosc.2009.12.011

Lee SJ, Sang JL, Lee YJ, Kim SB, Kim SK, Lee DW (2012) Homologous alkalophilic and acidophilic L-arabinose isomerases reveal region-specific contributions to the pH dependence of activity and stability. Appl Environ Microbiol 78(24):8813–8816. https://doi.org/10.1128/AEM.02114-12

Lim BC, Kim HJ, Oh DK (2007) High production of D-tagatose by the addition of boric acid. Biotechnol Prog 23(4):824–828. https://doi.org/10.1002/bp070056y

Long NVD, Le TH, Jinil K, Juweon L, Yoonmo K (2009) Separation of D-psicose and D-fructose using simulated moving bed chromatography. J Sep Sci 32(11):1987–1995. https://doi.org/10.1002/jssc.200800753

Marles-Wright J, Lewis RJ (2011) The structure of a D-lyxose isomerase from the σB regulon of *Bacillus subtilis*. Proteins 79(6):2015–2019. https://doi.org/10.1002/prot.23028

Mishra DK, Hwang JS (2013) Selective hydrogenation of D-mannose to D-mannitol using NiO-modified TiO 2 (NiO-TiO 2) supported ruthenium catalyst. Appl Catal A Gen 453(6):13–19. https://doi.org/10.1016/j.apcata.2012.11.042

Morita M, E S, K Y, Sakai T, Natori T, Koezuka Y, H F, K A (1996) Practical total synthesis of (2S,3S,4R)-1-O-(α-D-galactopyranosyl)-N-hexacosanoyl-2-amino-1,3,4-octadecanetriol, the antitumorial and immunostimulatory α-galactosylcer-amide, KRN7000. Biosci Biotechnol Biochem 60(2):288–292. https://doi.org/10.1271/bbb.60.288

Mozhaev VV (1993) Mechanism-based strategies for protein thermostabilization. Trends Biotechnol 11(3):88–95. https://doi.org/10.1016/0167-7799(93)90057-G

Okano K (2009) Synthesis and pharmaceutical application of L-ribose. Tetrahedron 65(10):1937–1949. https://doi.org/10.1016/j.tet.2008.11.047

Park CS, Kwon HJ, Yeom SJ, Oh DK (2010a) Mannose production from fructose by free and immobilized D-lyxose isomerases from *Providencia stuartii*. Biotechnol Lett 32(9):1305–1309. https://doi.org/10.1007/s10529-010-0300-2

Park CS, Kim JE, Choi JG, Oh DK (2011) Characterization of a recombinant cellobiose 2-epimerase from *Caldicellulosiruptor saccharolyticus* and its application in the production of mannose from glucose. Appl Microbiol Biotechnol 92(6):1187–1196. https://doi.org/10.1007/s00253-011-3403-3

Park CS, Yeom SJ, Lim YR, Kim YS, Oh DK (2010b) Substrate specificity of a recombinant D-lyxose isomerase from *Serratia proteamaculans* that produces D-lyxose and D-mannose. Lett in. Appl Microbiol 51(3):343–350. https://doi.org/10.1111/j.1472-765X.2010.02903.x

Patel DH, Wi SG, Lee SG, Lee DS, Song YH, Bae HJ (2011) Substrate specificity of the *Bacillus licheniformis* lyxose isomerase YdaE and its application in in vitro catalysis for bioproduction of lyxose and glucose by two-step isomerization. Appl Environ Microbiol 77(10):3343–3350. https://doi.org/10.1128/AEM.02693-10

Patel MJ, Akhani RC, Patel AT, Dedania SR, Patel DH (2017) A single and two step isomerization process for D-tagatose and L-ribose bioproduction using L-arabinose isomerase and D-lyxose isomerase. Enzym Microb Technol 97:27–33. https://doi.org/10.1016/j.enzmictec.2016.11.001

Shen SC, Wu JSB (2010) Maillard browning in ethanolic solution. J Food Sci 69(4):FCT273–FCT279

Swenson CA, Barker R (1971) Proportion of keto and aldehydo forms in solutions of sugars and sugar phosphates. Biochemistry 10(16):3151–3154. https://doi.org/10.1021/bi00792a026

Van LS, Park CS, Yeom SJ, Adamscioaba MA, Oh DK, Jia Z (2010) Structure-based annotation of a novel sugar isomerase from the pathogenic *E. coli* O157:H7. J Mol Biol 401(5):866–881

Vuksan V, Jenkins DJ, Spadafora P, Sievenpiper JL, Owen R, Vidgen E, Brighenti F, Josse R, Leiter LA, Bruce-Thompson C (1999) Konjac-mannan (glucomannan) improves glycemia and other associated risk factors for coronary heart disease in type 2 diabetes. A randomized controlled metabolic trial. Diabetes Care 22(6):913–919. https://doi.org/10.2337/diacare.22.6.913

Wagner N, Bosshart A, Failmezger J, Bechtold M, Panke S (2015) A separation-integrated cascade reaction to overcome thermodynamic limitations in rare-sugar synthesis. Angew Chem Int Edit 54(14):4182–4186. https://doi.org/10.1002/anie.201411279

Xu W, Zhang W, Zhang T, Jiang B, Mu W (2016a) L-rhamnose isomerase and its use for biotechnological production of rare sugars. Appl Microbiol Biotechnol 100(7):1–8

Xu Z, Li S, Feng X, Liang J, Xu H (2014) L-arabinose isomerase and its use for biotechnological production of rare sugars. Appl Microbiol Biotechnol 98(21):8869–8878. https://doi.org/10.1007/s00253-014-6073-0

Xu Z, Sha Y, Liu C, Li S, Liang J, Zhou J, Xu H (2016b) L-ribose isomerase and mannose-6-phosphate isomerase: properties and applications for l-ribose production. Appl Microbiol Biotechnol 100(21):9003–9011. https://doi.org/10.1007/s00253-016-7834-8

Takagi Y, Nakai K, Tsuchiya T, Takeuchi T (1996) A 5′-(Trifluoromethyl)anthracycline glycoside: synthesis of antitumor-active 7-O-(2,6-Dideoxy-6,6,6-trifluoro-α-l-lyxo-hexopyranosyl)adriamycinone. J Med Chem 39(8):1582–1588

Yeom SJ, Ji JH, Kim NH, Park CS, Oh DK (2009) Substrate specificity of a mannose-6-phosphate isomerase from *Bacillus subtilis* and its application in the production of L-ribose. Appl Environ Microbiol 75(14):4705–4710. https://doi.org/10.1128/AEM.00310-09

Yu L, Zhang W, Zhang T, Jiang B, Mu W (2016) Efficient biotransformation of D-fructose to D-mannose by a thermostable D-lyxose isomerase from *Thermosediminibacter oceani*. Process Biochem 51(12):2026–2033. https://doi.org/10.1016/j.procbio.2016.08.023

Zhang D, Chia C, Jiao X, Jin W, Kasagi S, Wu R, Konkel JE, Nakatsukasa H, Zanvit P, Goldberg N, Chen Q, Sun L, Chen ZJ, Chen W (2017a) D-mannose induces regulatory T cells and suppresses immunopathology. Nat Med 23(9):1036–1045. https://doi.org/10.1038/nm.4375

Zhang W, Fang D, Xing Q, Zhou L, Jiang B, Mu W (2013) Characterization of a novel metal-dependent D-psicose 3-epimerase from *Clostridium scindens* 35704. PLoS One 8(4):e62987. https://doi.org/10.1371/journal.pone.0062987

Zhang W, Li H, Zhang T, Jiang B, Zhou L, Mu W (2015) Characterization of a D-psicose 3-epimerase from *Dorea* sp. CAG317 with an acidic pH optimum and a high specific activity. J Mol Catal B Enzym 120: 68–74. https://doi.org/10.1016/j.molcatb.2015.05.018

Zhang W, Yu S, Zhang T, Jiang B, Mu W (2016) Recent advances in D-allulose: physiological functionalities, applications, and biological production. Trends Food Sci Technol 54:127–137. https://doi.org/10.1016/j.tifs.2016.06.004

Zhang W, Zhang T, Jiang B, Mu W (2017b) Enzymatic approaches to rare sugar production. Biotechnol Adv 35(2):267–274. https://doi.org/10.1016/j.biotechadv.2017.01.004